AAS 05-002


# Line of Sight Stabilization of James Webb Space Telescope

Luis Meza, Frank Tung, Satya Anandakrishnan
Northrop Grumman Space Technology

Victor Spector
GeoLogics

Tupper Hyde
NASA GSFC

**27th ANNUAL AAS GUIDANCE AND CONTROL CONFERENCE**

February 5-9, 2005
Breckenridge, Colorado

Sponsored by
Rocky Mountain Section

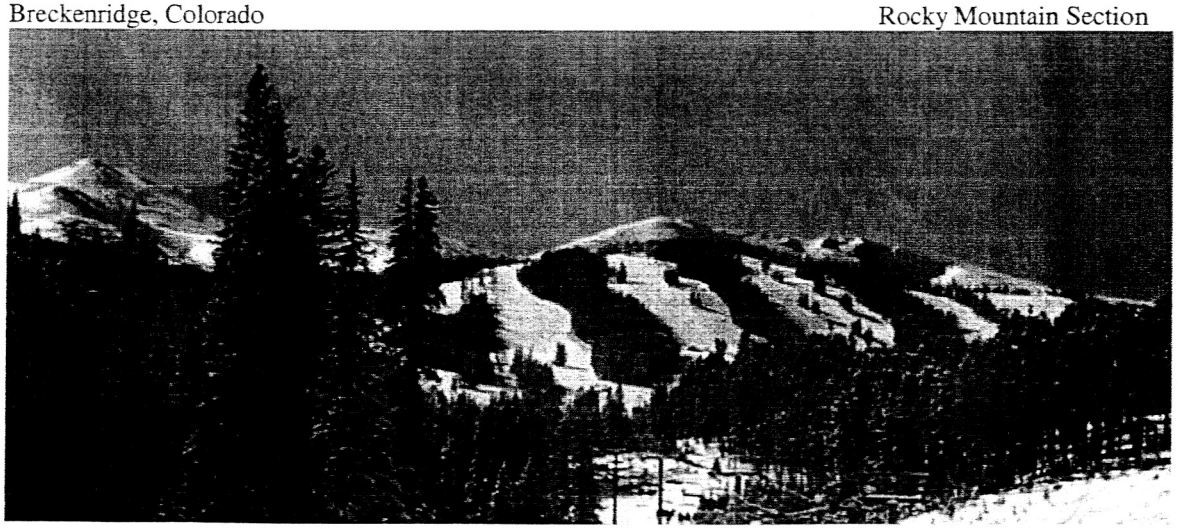

AAS Publications Office, P.O. Box 28130 - San Diego, California 92198

AAS 05-002

# Line Of Sight Stabilization for the James Webb Space Telescope

**Luis Meza, Frank Tung, Satya Anandakrishnan, Victor Spector, and Tupper Hyde**

The James Webb Space Telescope (JWST) builds upon the successful flight experience of the Chandra Xray Telescope by incorporating an additional LOS pointing servo to meet the more stringent pointing requirements. The LOS pointing servo, referred to in JWST as the Fine Guidance Control System (FGCS), will utilize a Fine Guidance Sensor (FGS) as the sensor, and a Fine Steering Mirror (FSM) as the actuator. The FSM is a part of the Optical Telescope Element (OTE) and is in the optical path between the tertiary mirror and the instrument focal plane, while the FGS is part of the Integrated Science Instrument Module (ISIM).

The basic Chandra spacecraft bus attitude control and determination architecture, utilizing gyros, star trackers/aspect camera, and reaction wheels, is retained for JWST. This system has achieved pointing stability of better than 0.5 arcseconds. To reach the JWST requirements of milli-arcsecond pointing stability with this ACS hardware, the local FGCS loop is added to the optical path. The FGCS bandwidth is about 2.0 Hz and will therefore attenuate much of the spacecraft ACS induced low frequency jitter. In order to attenuate the higher frequency (> 2.0 Hz) disturbances associated with reaction wheel static and dynamic imbalances, as well as bearing run-out, JWST will employ a two-stage passive vibration isolation system consisting of (1) 7.0 Hz reaction wheel isolators between each reaction wheel and the spacecraft bus, and (2) a 1.0 Hz tower isolator between the spacecraft bus and the Optical Telescope Element (OTE).

In order to sense and measure the LOS, the FGS behaves much like an autonomous star tracker that has a very small field of view and uses the optics of the telescope. It performs the functions of acquisition, identification and tracking of stars in its 2.5 x 2.5 arcminute field of view (FOV), and provides the centroid and magnitude of the selected star for use in LOS control. However, since only a single star is being tracked at any time within the FGS FOV there is only tip and tilt information; rotation about the FGS LOS will not be sensed. The FGCS uses the FSM to move the guide star within the FGS FOV and place the centroid of the guide star at any desired position within the FGS focal plane. Using this architecture allows the FGCS to correct the low frequency LOS jitter that is induced by the spacecraft ACS in pitch and yaw, and achieve the milli-arcsecond pointing stability required by JWST. The less stringent ISIM FOV roll performance will be provided solely by the ACS, using the spacecraft gyros and star trackers. Since the FSM is in the optical path, the pointing stability of a science object in any of the instruments will be similar to that of the guide star LOS.

## INTRODUCTION

Following its planned 2011 launch, the NASA James Webb Space Telescope (JWST) will be the premier space based infrared program for astrophysics. JWST will observe red shifted light from the early universe, including the period when the first stars and galaxies began to form. JWST is being instrumented for imaging and spectroscopy, with better than 100 milli-arcsecond (mas) resolution, nano-Jansky sensitivity, and a large field of view. The JWST Observatory will orbit about the second Lagrange point (L2). NASA Goddard Space Flight Center (GSFC) manages JWST with contributions from a team of academic, government, and industrial partners.

The contract to build the space-based JWST Observatory was awarded to the Northrop Grumman Space Technology (NGST)/Ball/ITT/ATK team.

The Observatory (Figure 1) is composed of: the OTE, ISIM, and the spacecraft element. The SpaceCraft Element (SCE) includes the spacecraft bus and the sunshield. The OTE is a deployable optical system with diffraction limited performance at 2 $\mu$m and a stable point spread function (PSF). The ISIM consists of four Science Instruments (SIs): 1) a Near-InfraRed (0.6 to 5 $\mu$m) Camera – NIRCam, 2) a Near-InfraRed (0.6 to 5 $\mu$m) multi-object Spectrograph- NIRSpec, 3) a Mid- InfraRed (5 to 30 $\mu$m) Imager- MIRI, and 4) a Tunable Filter (0.6 to 5$\mu$m) camera – FGS/TF. The ISIM also contains a fine guidance sensor FGS as part of the FGS/TF.

The spacecraft bus (Figure 2) provides a stable pointing platform and housekeeping functions for the Observatory. The sunshield shades the OTE and ISIM from solar illumination to allow operation with high sensitivity past 27 $\mu$m, and provides a stable thermal environment for the OTE/ISIM.

The spacecraft attitude control system uses gyros and star trackers as sensors and reaction wheels as control actuators. This equipment will meet the coarse pointing requirements of 7 arcseconds pointing accuracy and pointing stability of 1 arcsecond over each 0.1 second period. The less stringent ISIM FOV roll performance will be provided solely by the spacecraft ACS.

A two-stage passive vibration isolation system will be used to attenuate higher frequency (>2.0 Hz) disturbances associated with reaction wheel static and dynamic imbalances, as well as bearing run-out. Stage 1 isolation consists of 7.0 Hz reaction wheel isolators located between each reaction wheel and the spacecraft bus, while stage 2 is a 1.0 Hz tower isolator between the spacecraft bus and the OTE.

In addition to the isolation system, in order to meet the sub arcsecond JWST LOS pointing requirements, a local LOS pointing servo is required to stabilize the LOS in the ISIM FOV. The LOS pointing servo, the FGCS, utilizes the FGS as the sensor, and the FSM as the actuator. Both of these are placed within the JWST optical path: the FSM between the tertiary mirror and the instrument focal plane, and the FGS at the instrument focal plane. The FGCS bandwidth is about 2.0 Hz and will, therefore, attenuate much of the spacecraft ACS induced low frequency jitter. This paper will focus only on the FGCS design and performance.

The FGS, provided by the Canadian Space Agency, performs the functions of acquisition, identification and tracking of stars in its FOV, and provides the centroid and magnitude of the selected star for use in control. The FGCS uses the FSM to move the guide star within the FGS FOV and place the centroid in the desired position within the FGS focal plane. Using this architecture allows the FGCS to correct the low frequency LOS jitter that is induced by the spacecraft ACS in pitch and yaw, and achieve the milli-arcsecond pointing stability required by JWST.

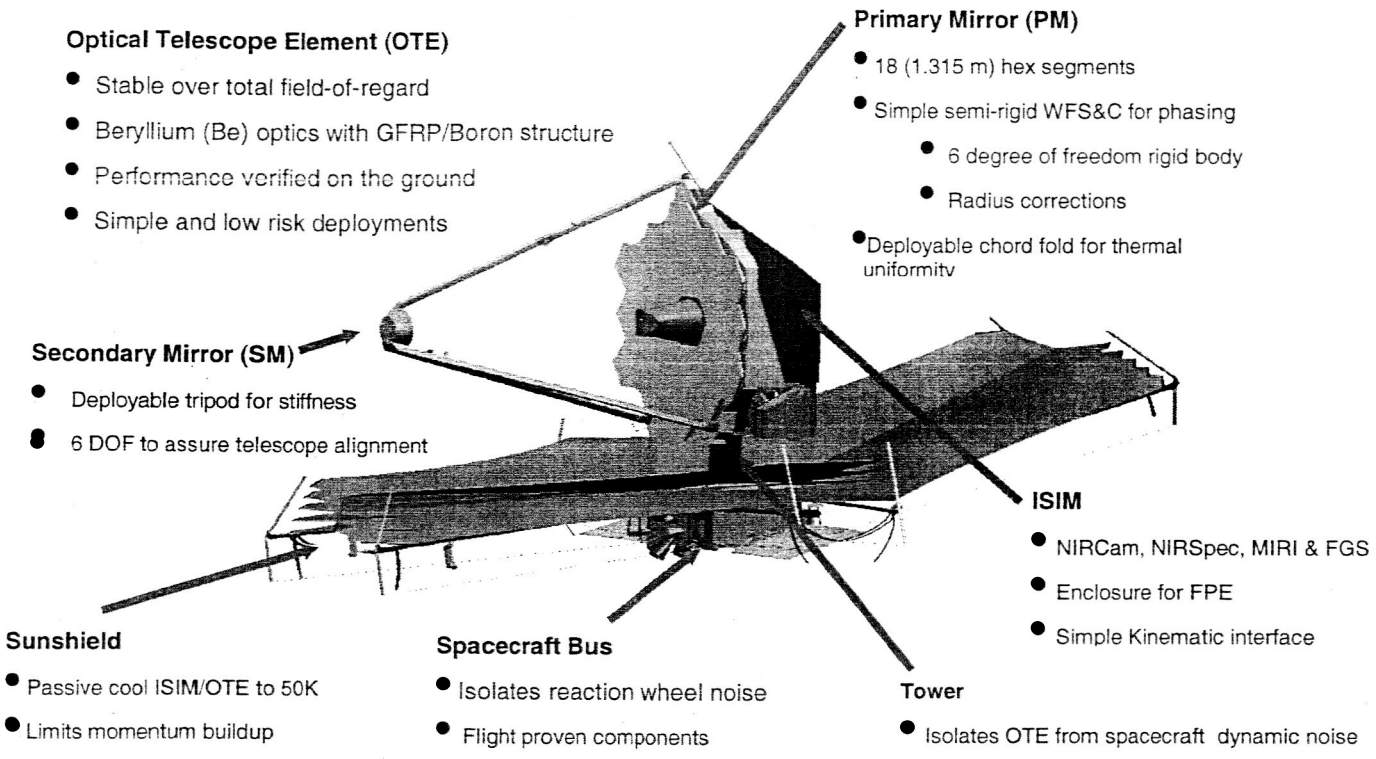


**Figure 1: James Webb Space Telescope**

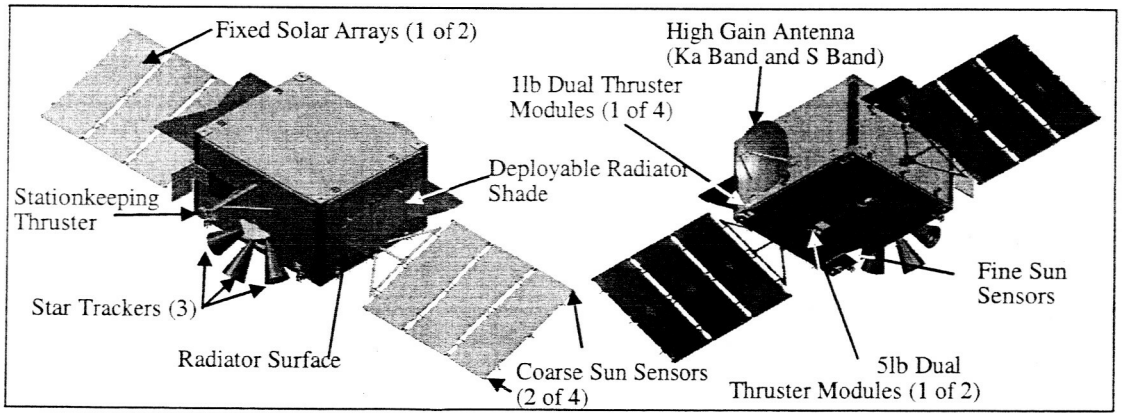


**Figure 2: JWST Spacecraft External Configuration**

## OVERVIEW OF ATTITUDE CONTROL SUBSYSTEM

The ACS subsystem provides spacecraft attitude determination and control, and fine control of the telescope LOS. In addition the ACS subsystem is responsible for slew maneuvers, momentum unloading, thrust vector pointing, delta-v maneuver control, high gain antenna (HGA) pointing, and backup control modes that support contingency management. Figure 3 shows the ACS subsystem hardware block diagram.

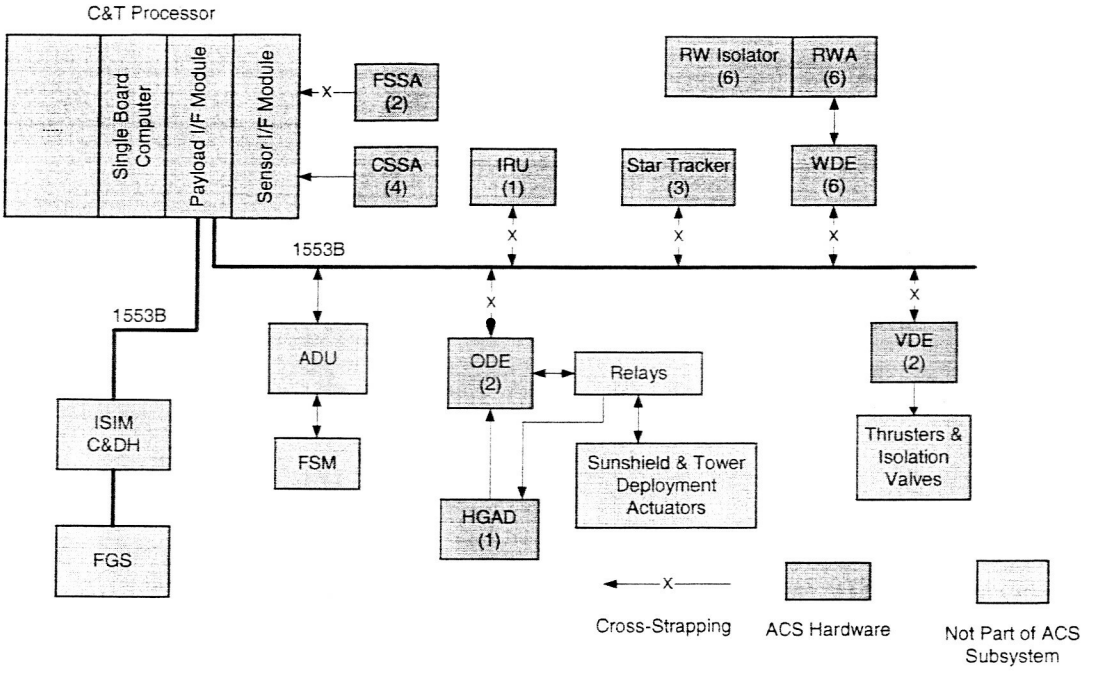


**Figure 3: ACS Subsystem Hardware Block Diagram**

The ACS avionics suite of sensors and actuators consists of 3 star tracker assemblies (STA), 1 internally redundant inertial reference unit (IRU), 2 fine sun sensors (FSS), 4 coarse sun sensors, 6 sets of reaction wheels (RWA) and isolators (RW Isolator) in a pyramidal configuration, 1 bi-axial high gain antenna drive, and thrusters for momentum unloading and delta-v.

ACS software is implemented in a single board computer (SBC) within the command and telemetry processor (CTP). Sensor and actuator communications are through a 1553 data bus. The ISIM processor provides guide star centroid data to the CTP. Based on the ACS commands from the SBC, via the CTP, the actuator drive unit (ADU) drives the FSM actuators.

The Key ACS requirements are listed in Table 1. The ACS controls Observatory slews per commands from the ISIM. An Euler angle slew profile is used to keep the sun within allowable region during slew. Star trackers provide star measurements during the slew for attitude updates–improving accuracy and reducing the transient at the end of the slew. Before

enabling the Fine Guidance Control System, the spacecraft attitude control system can point the telescope to within 6.5 arcsec (1-sigma, per axis). This is referred to as coarse pointing. Coarse pointing provides sufficient accuracy for the FGS to identify and acquire guide star.

**Table 1: Key ACS Requirements**

| |
|---|
| **Telescope Line of sight motion < 3.7 mas** |
| **Coarse pointing stability < 1 arcsec over 0.1 sec** |
| **Roll stability about the optical axis < 0.8 arcsec (1 sigma) during an exposure frame** |
| **Coarse roll control < 6.4 arcsec (1 sigma per axis)** |
| **Roll alignment shift < 3.7 mas (1 sig, per axis) in 24 hours** |
| **Slew rates: 90 deg in < 56.5 minutes,**<br>**280 arc-sec slew in < 6 min,**<br>**20 arc-sec slew in < 40 sec** |
| **Spacecraft roll shift for FOV Offsets:**<br>**0.0 - 0.5 arcsec +/- 0.7 arcsec**<br>**0.5 – 2.0 arcsec +/- 2.0 arcsec**<br>**2.0 – 20.0 arcsec +/- 3.0 arcsec** |
| **Coarse pointing accuracy < 6.5 arc-sec (1 sigma per axis)** |
| **HGA pointing < 0.13 deg (3-sigma, radial)** |

During fine guidance, the Observatory level Image Motion requirement is 7 mas (1-sigma, per axis), driven by optical wave front error requirements. The observatory level image motion requirement is sub-allocated by frequency (see Figure 4) to high frequency (above FGCS bandwidth), low frequency (within FGCS bandwidth) and very low frequency (below FGCS bandwidth – mainly due to deformations caused by thermal gradients). The low frequency image motion, or the LOS jitter, is of interest to the FGCS, and is further sub-allocated to three sources. The first source, ACS roll about LOS, is a result of the fact that a roll about the guide star LOS will result in jitter of the image in the SI, which can be as much as 10.2 arcminutes (NIRCam, the most sensitive to wave front error) from the guide star. The second source, FSM induced smear, accounts for the affect of differential distortion due to the motion of the FSM. The third source is directly attributable to the FGCS and is driven by the command resolution of the FSM, the noise in the FGS centroid data, and disturbance from the spacecraft bus that is not isolated by the tower isolator. Figure 4 shows the Image Motion error budget, which allocates 3.7 mas to the Fine Guidance Control System.

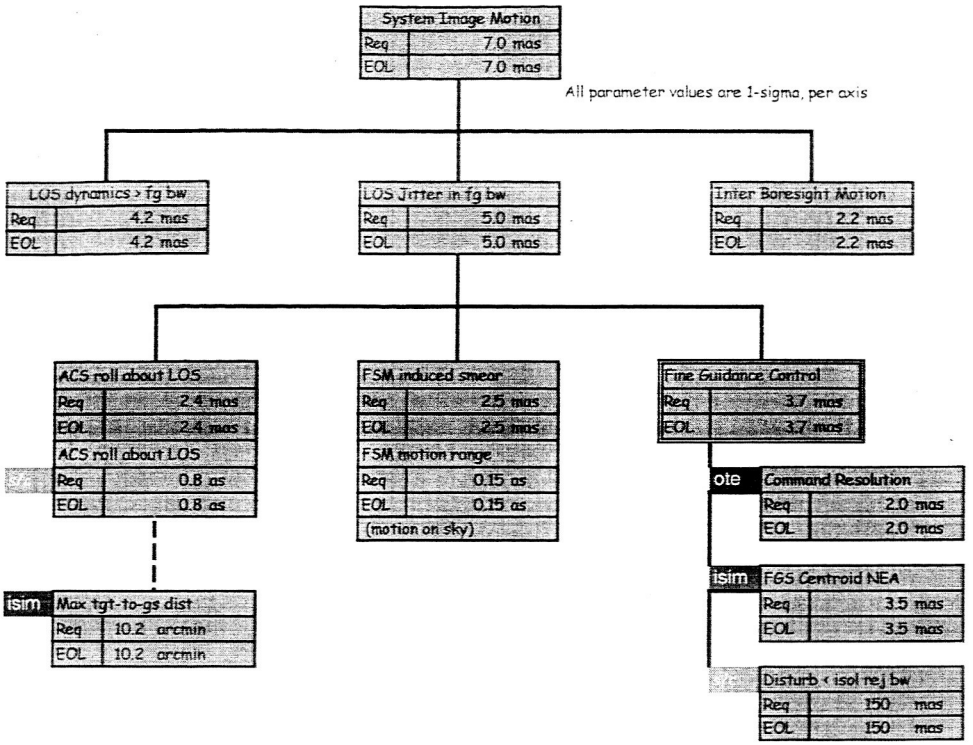


**Figure 4:System Image Motion Error Budget Allocates 3.7 mas to Fine Guidance Control System.**

## POINTING CONTROL SYSTEM DESIGN APPROACH

Design of the Pointing Control System (PCS) begins by modeling and analyzing the control loops using Matlab in the frequency domain to meet certain stability and disturbance rejection properties. The control loop topology is then modeled in the time domain using Simulink to verify control performance in the presence of system nonlinearities such as quantizations, sampling effects, and saturations. Figure 5 shows the integrated design cycle for the pointing control loop design.

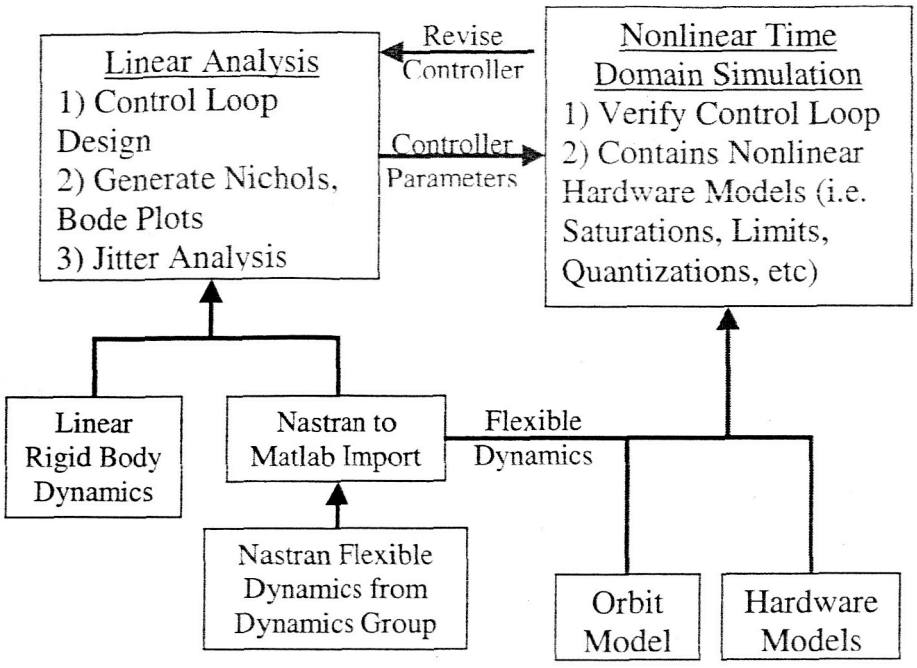


**Figure 5: Integrated Modeling Architecture and Design Cycle for Attitude Control System**

## POINTING CONTROL SYSTEM ARCHITECTURE

The JWST Pointing Control System (PCS) is comprised of three integrated control systems: 1) a 3-axis, low bandwidth (0.02Hz) inertial referenced spacecraft attitude control system (ACS) for coarse attitude control; 2) a 2-axis, high-bandwidth (2Hz) telescope line-of-sight (LOS) stabilization control system using a Fast Steering Mirror (FSM); and 3) a 2-axis, very low bandwidth (0.004Hz) FSM Offloading control system. A concise but detailed interaction between these three main control systems, the required sampling times, the handshaking between the Spacecraft SBC and ISIM On-Board-Computer (OBC), and their connection to the real world is shown in Figure 6.

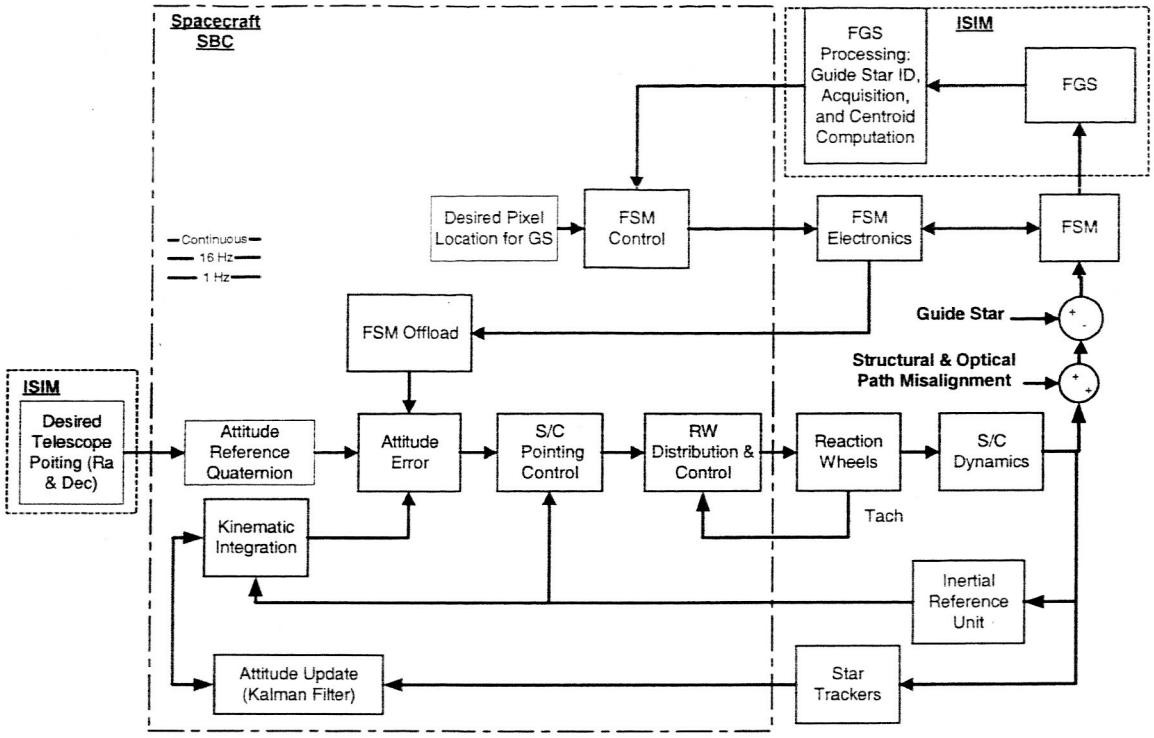


**Figure 6: Integrated Pointing Control Architecture Showing the ACS topology (bottom loop: S/C Pointing Control, RW, IRU and STA), the FGCS (top loop: FSM control, FSM, FGS), and the connection of the FGCS and the ACS through the FSM Offloading loop.**

## ATTITUDE CONTROL SYSTEM

The JWST ACS utilizes star trackers and IRU's for attitude determination, and RWAs for control. The ACS loop topology per axis consists of a Proportional+Integral+Derivate (PID) compensator, a second order bending filter to attenuate flexible modes, a momentum control loop for reaction wheel control, and an IRU (4Hz bandwidth) for body rate information. The on-board attitude information is maintained and propagated as quaternions, by performing the kinematic integration using IRU data at every SBC minor cycle (0.064sec). In addition, a Kalman filter, running at a slower rate (1.024 sec), is used to correct the IRU drift and the SBC attitude quaternion by using star tracker measurements referenced to a star catalog.

The momentum exchange system consists of a 6 RWAs configured in a pyramid configuration to provide balanced momentum storage capability in each of the three spacecraft axes. The momentum control loop consists of a Proportional+Integral (PI) compensator, a first-order low-pass filter, a tachometer, and a tachometer-averaging filter for each wheel. The tachometer provides reaction wheel speed measurements at the quantization level of 19.5rpm, based on its 48 pulses-per-revolution (ppr) performance and 0.064 sec readout rate. The reaction wheels are speed biased to 2700rpm by using an additional bias control loop that regulates reaction wheel speed operation near a fixed speed in the null-space of the RWA cluster. This RW speed bias set point is needed to maintain RW speeds within an acceptable speed range of 15Hz to 75Hz in order to avoide structural excitations that may contribute to LOS jitter. The momentum and bias control loop bandwidths are set to 0.2Hz and 0.008Hz respectively

### Fine Guidance Control System

The Fine Guidance Control system (FGCS) bandwidth is approximately 2Hz in order to effectively remove ACS jitter, and utilizes guide star information processed and accessed by the ISIM to acquire and track desired targets in the ISIM FOV using the FSM. The ISIM contains an FGS that is used to report Guide Star locations in its focal plane to within 3.5 mas (NEA). The Fine Guidance Loop consists of a PID compensator, a second-order bending filter to improve sensor noise rejection, an FSM to provide corrections to the LOS, and a dedicated FGS. The FGS is used to acquire and lock onto the desired guide star (GS) thereby stabilizing the complete ISIM FOV where the science targets are being exposed.

The FGS uses only one guide star for control. Therefore, the FGCS cannot control the roll axis, and controls only two the pitch and yaw LOS motion.

## FSM OFFLOADING LOOP

The FSM Offloading Loop bandwidth is 0.004Hz and serves to maintain the FSM position about it's null setting in order to reduce FSM induced image smear. The FSM Offloading Loop consists of a PI controller that adds the FSM position (through the PI compensator) as a bias to the attitude error signal. Note that a coordinate transformation from optical to spacecraft coordinates is needed prior to biasing the ACS error signal.

## CONTROL LOOP DESIGN AND ANALYSIS

The control loop design for the ACS, FGCS and the FSM Offloading is done using continuous linear hardware models and dynamics in the Matlab environment. The control loops are analyzed and designed in the frequency domain using Nichols and Bode plots. Refer to Table 1 for loop performance and margins. The ACS is analyzed as a PID controller, a second order bending filter, a momentum control system, linear rigid and flexible dynamics, and a second order IRU model. The momentum control loop is an embedded 0.2Hz bandwidth control system that is represented by a PI, a first order low pass filter, and linear reaction wheel dynamics. The IRU is modeled as a second order system with un-damped natural frequency of 4Hz and damping ratio of 0.87. The FGCS is analyzed and designed using a PID, a first order low pass filter, and linearized FSM dynamics. The FSM Offloading Loop connects the FSM position through a PI controller to the ACS attitude error.Table 2 lists the results of the linear stability analyses for the three loops. Figures 3 and 4 show the open loop Nichols plots for the ACS and FSM offloading loops.

**Table 2: Pointing Control – Loop Performance**

| | Roll | Pitch | Yaw |
|---|---|---|---|
| ACS | | | |
| - Bandwidth, Hz | 0.02 | 0.02 | 0.02 |
| - Gain Margin, dB | 12 | 12 | 12 |
| - Phase Margin, deg | 60 | 60 | 60 |
| FSM FGCS | | | |
| - Bandwidth, Hz | N/A | 2 (V2 Axis) | 2 (V3 Axis) |
| FSM Offloading | | | |
| - Bandwidth, Hz | 0.004 | 0.004 | 0.004 |
| - Gain Margin, dB | 15 | 15 | 15 |
| - Phase Margin, deg | 90 | 90 | 90 |

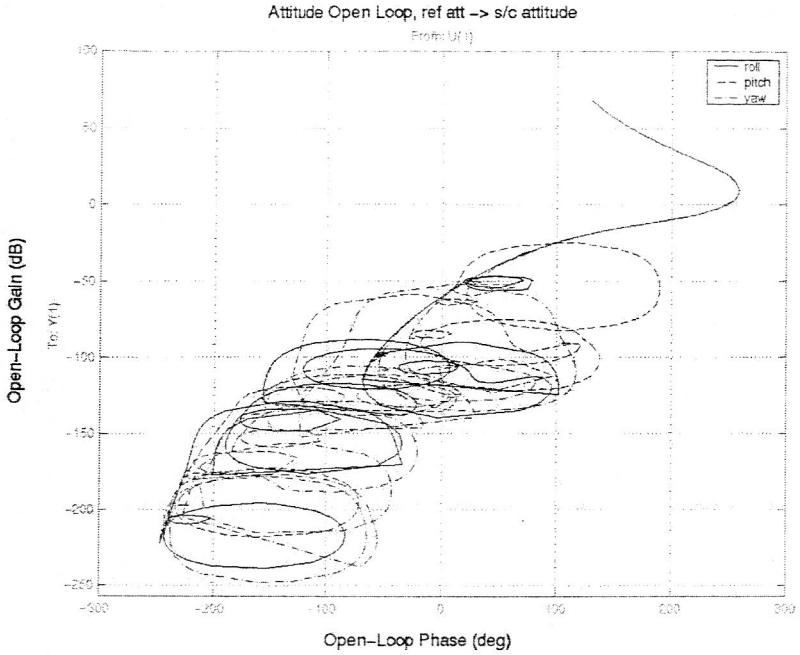


**Figure 7: ACS Nichols Plot Shows Stability Margins in the Presence of Flexible Dynamics.**

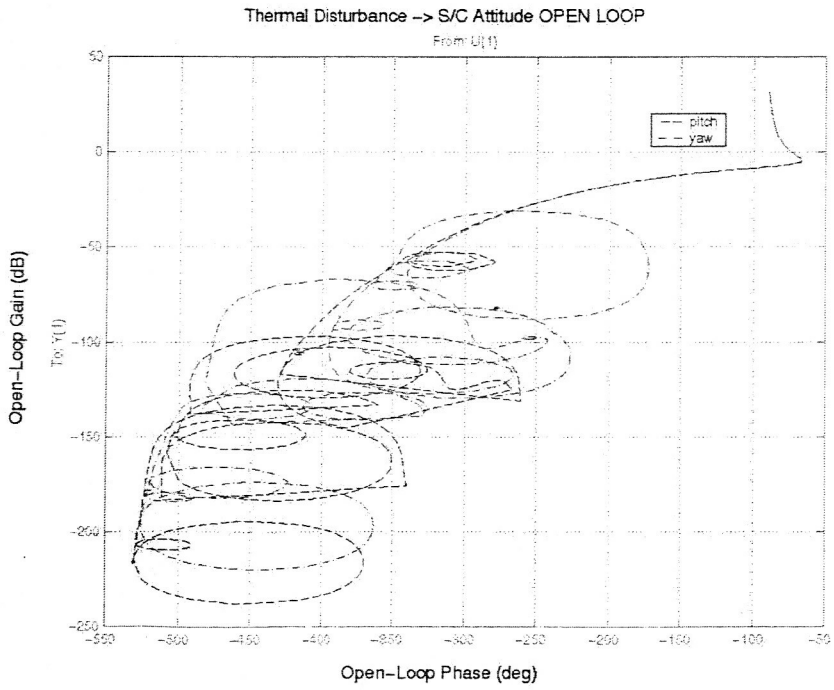


**Figure 8: Nichols Plot for FSM Offloading Loop Shows Stability Margins in the Presence of Flexible Dynamics.**

The FSM bandwidth of 2Hz was chosen based on the FGS noise characteristics and mission requirements of using a faint guide star (magnitude 18) for guiding. The acceptable NEA for guiding was chosen as 42% of the LOS pointing stability requirement of 7mas, resulting in a 3mas NEA requirement. Figure 9 shows the FGS NEA as a function of sample rate (1/integration time) for various star magnitudes. It can be seen that in order to meet the 3mas NEA for a 18 magnitude guide star the maximum sample rate is 20Hz. The parameters affecting the NEA are the wavelength, bandpass, dark current, read noise, guide box, encircled energy requirement, and plate scale. The FSM bandwidth is then chosen in conjunction with the maximum FGS sample rate to maintain a sample rate to bandwidth ratio of 10:1.

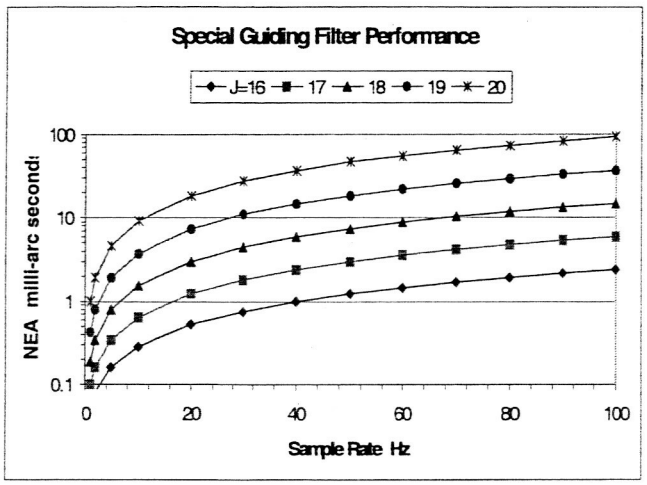


**Figure 9: Noise Equivalent Angles as function of sample rate (1/integration_time) for different Star Magnitudes**

## TIME DOMAIN SIMULATION

The JWST ACS simulation is based on CXO's Pointing Control and Attitude Determination (PCAD) subsystem. The ACS hardware models such as the reaction wheels, reaction wheel speed tachometer, reaction wheel disturbance models, and inertial reference units (IRU's) are all taken CXO. Refer to Table 3 for hardware parameter settings. In addition, to accurately represent the complete pointing control system, the FGCS and FSM Offloading loops, with their associated nonlinearities, have been added.

## POINTING CONTROL HARDWARE MODELS

The required pointing control hardware consists of sensors (star trackers, IRU, FGS), and actuators (reaction wheels, FSM) whose input and output signals are converted and passed as counts. Except for the FGSandFSM, the sensor models are directly taken from CXO and converted to a Matlab/Simulink equivalent.

The star tracker is modeled having a rectangular 8° x 8° FOV, containing 5 stars, all of which are corrupted by Gaussian noise. In addition the measurement residual between the measured and the estimated star locations are computed and sent to the Kalman Filter at a specified rate. The IRU is modeled as one gyro per axis, with an integrated rate quantization of 0.05 arcsec/count. In addition, the IRU input rate is corrupted by three components: 1) a static bias term, 2) a rate random walk component, and 3) an angle random walk component. The FGS

is currently represented as a quantized centroid error with additive Gaussian noise to represent centroiding quantization at the FGS and detector noise. Continuous linear models represent the reaction wheels with coulomb and viscous friction in the feedback. The torque on the spacecraft is found by the appropriate transformations, which relate the torque on the spin axis and the disturbance torques due to dynamic imbalances in the transverse axes. Similarly, the reaction wheel disturbance forces due to static imbalances in the transverse axes, and bearing imperfections in the spin axis are transformed. The FSM is represented as a linear transfer function with torque-input quantization, and FSM mirror position quantization output.

## POINTING CONTROL SOFTWARE

The SBC software is digitally represented by using discrete transfer function blocks in Simulink to model the control loop topology, except for the slew maneuver, star tracker and Kalman filter which are written in C and embedded as CMEX S-Functions. The control loop gains are computed using linearized models in the frequency domain and are then used in the control laws in digital form. The multi-rate transitions are handled and regulated by Simulink by using equivalent sample and hold blocks to transition from the digital to the continuous and from the continuous to the digital domains.

## SPACECRAFT DYNAMICS

The JWST spacecraft dynamics are modeled as a true rigid body corrupted by flexible contributions. The rigid body spacecraft dynamics are represented by Euler's equations of motion $\dot{\underline{H}} + \underline{w} \times \underline{H} = \underline{T}$, where $\underline{H}$ is the spacecraft angular momentum vector, $\underline{w}$ is the angular rate vector, and $\underline{T}$ is the torque vector applied by the reaction wheels. The flexible dynamics are represented by a state-space model, which is constructed using the mass-normalized eigenvalues of the observatory finite element model (FEM) based on modal analysis. The flexible dynamics model is delivered to ACS from the dynamics group, with several available input-output nodes in the FEM such as the reaction wheel disturbance inputs and some desired outputs such as vibration at spacecraft c.g., and line of sight jitter. The resulting model is of the form $\dot{\underline{x}} = \underline{Ax} + \underline{BU}$ with output equations $\underline{y} = \underline{Cx}$ for the desired output nodes, and $WFE = \| \underline{Sx} \|_2$ for the wavefront error, where $\underline{S}$ is the sensitivity matrix and || represent the Euclidean norm.

The rigid body spacecraft angular rate is then used in a continuous kinematic integration to obtain the true spacecraft attitude as a quaternion. The spacecraft rates used for input to the gyro for performing the on-board attitude propagation consists of the addition of the rigid and flexible body angular rates; *the* bus c.g. output nodes are chosen as the truth model corruption due to structural flexibility as the IRU model input). The onboard attitude propagation is performed at every SBC minor cycle of 64msec.

**Table 3: Hardware parameters used for JWST Pointing Control Simulation**

| Hardware | Parameter | Value | Units |
|---|---|---|---|
| Reaction Wheels | | | |
| | Inertia | 0.1295 | Kg-m$^2$ |
| | Coulomb Friction | 0.0050 | N-m / rad |
| | Viscous Friction | 2.1241e-005 | N-m / (rad/sec) |
| | Static Imbalance | 1.0787e-005 | N / (rad/sec) |
| | Dynamic Imbalance | 2.0107e-006 | N-m / (rad/sec) |
| | Bearing Imperfection | 2.0107e-006 | N / (rad/sec) |
| | Command Quantization | 0.0011 | N-m |
| | Maximum Speed | 6000 | Rpm |
| | Maximum Torque | 0.12 | N-m |
| Tachometer | | | |
| | Pulses per Revolution | 48 | - |
| | Sampling | 0.064 | Sec |
| | Number of A/D Bits | 16 | - |
| IRU | | | |
| | Bandwidth | 4 | Hz |
| | Damping Factor | 0.87 | - |
| | Quantization | 0.02 | arc-second |
| | Angle Random Walk | 0.019 | arc-second /sec^(1/2) |
| | Rate random walk | 1.33e-5 | arc-second /sec^(3/2) |
| | Bias | 0.001 | arc-second/sec |
| | Number of A/D Bits | 16 | - |
| Star Tracker | | | |
| | Field of View | 8° x 8° | Degrees |
| | Star Tracker Noise (1□) | 2.6 | arc-second |
| | Alignment Euler Angles w.r.t. Spacecraft | [0 ; 45; 0] | Degrees |
| Fine Steering Mirror | | | |
| | Inertia | 0.0014 | Kg-m$^2$ |
| | Position Quantization | 0.002 | arc-second |
| | Torque Quantization | 3.23e-7 | N-m |
| Fine Guidance Sensor | | | |
| | Centroid Quantization | 3 | Mas |
| | Centroid Noise (1□) | 3 | Mas |
| Spacecraft | Inertia Tensor | [67946 -83 11129<br>-83 90061 103<br>11129 103 45821 ] | Kg-m$^2$ |

## POINTING CONTROL SIMULATION RESULTS

The JWST pointing performance is then obtained and validated by using the developed non-linear time simulation. The two results of interest are the spacecraft attitude and Corrected Line of Sight Stability. The corrected line of sight (centroid error) is shown in Figure 10 where it can be seen that the jitter is within requirements (see Table 1). The spacecraft attitude is shown in Figure 11, where the spacecraft pointing stability definitely meets the derived requirements (see Table 1) to minimize field distortions due to FSM compensation.

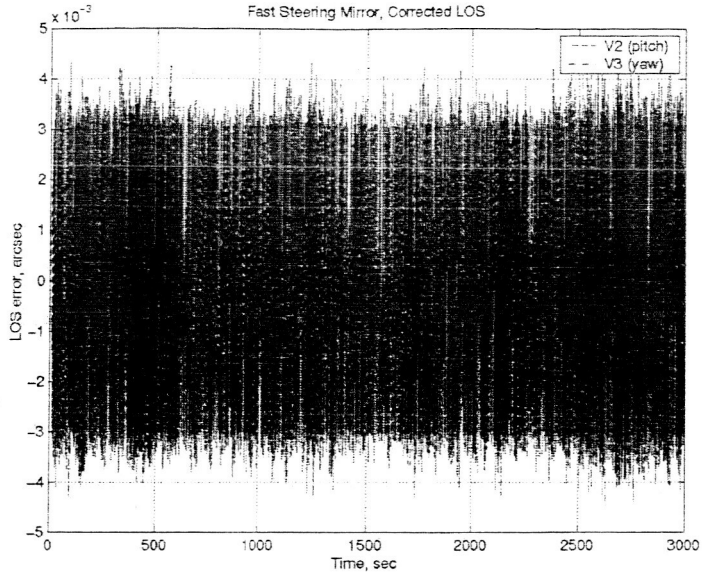


**Figure 10: Corrected Line of Sight at Focal Plane using JWST Pointing Control System.**

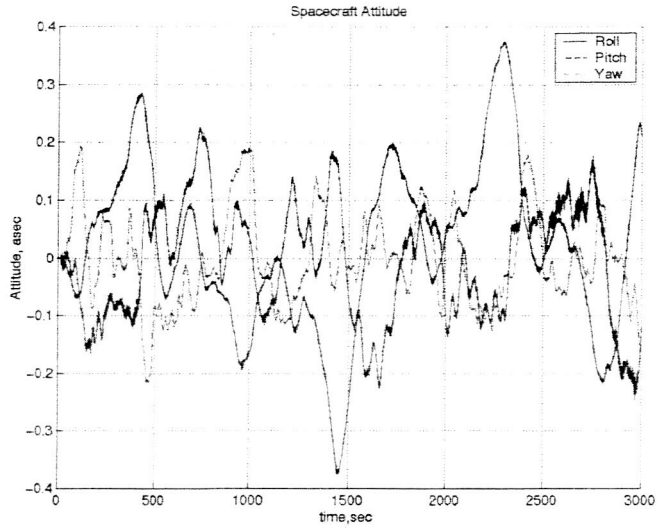


**Figure 11: Spacecraft Pointing Stability during Fine Guidance meets derived requirements of 1 arcsec (1σ) roll, and 0.12 arcsec (1σ) pitch and yaw.**

## ACKNOWLEDGEMENTS

Work was supported in part by the JWST contract NAS5-02200 with NASA GSFC. The JWST system is a collaborative effort involving NASA, ESA, CSA, the Astronomy community and numerous principal investigators.